AUNE, R.E., HAYASHI, M. and SRIDHAR, S. A thermodynamic approach to physical properties of silicate melts. *VII International Conference on Molten Slags Fluxes and Salts,* The South African Institute of Mining and Metallurgy, 2004.

A thermodynamic approach to physical properties of silicate melts

R.E. AUNE*, M. HAYASHI* and S. SRIDHAR†

*Royal Institute of Technology, Department of Materials Science and Engineering, Stockholm, Sweden

†Carnegie Mellon University, Department of Materials Science and Engineering, Pittsburgh, USA

Thermophysical properties of silicate melts are strongly structure dependent. It is wellknown that the viscosities of slags increase with increasing the degree of polymerization of silicate anions. Even the thermodynamic properties of slags are dependent on the types of species and the population of the same in the melt. Thus, a link between the thermophysical and thermochemical properties of silicate melts is logically expected.

The present paper elucidates the salient features of Darken's excess stability approach to the Gibbs energies of solutions as applied to the viscosities of silicate melts. It is demonstrated, that the second derivatives of the viscosities of binary silicate melts with respect to composition indicate a maxima corresponding to the existence of stable compounds in these systems. The concept was successfully applied to the following systems: Al_2O_3-SiO_2, CaO-SiO_2, FeO-SiO_2, MgO-SiO_2 and MnO-SiO_2. In all the cases, the second derivative plots of viscosities with respect to composition showed peaks corresponding to the metasilicates.

The second derivatives of the activation energies of viscous flow with respect to temperature has earlier been shown to reflect the formation of associates/embryos in the homogeneous silicate melts, indicating the readiness of the melt to separate a solid phase.

Thermodynamic coupling of thermal diffusivities in the case of the system CaO-Al_2O_3-SiO_2 from the laser-flash measurements of these slags as a function of temperature are examined as part of the present study. Densities are estimated from integral molar enthalpies in the case of silicate systems and the results are presented.

Keywords: silicate melts, viscosity; activation energy, thermal diffusivity; density

Introduction

In scientific history, the understanding of the structure of materials has mainly been through studies of different properties. Structure-based calculations of system properties have, over the years, only been met with limited success as they have been restricted to specific compositional and/or temperature ranges. As a result of this, experimental measurements of different system properties have become more and more important. It is important to point out, however, that efforts have mainly focused on two distinct types of properties, that is thermophysical and thermochemical properties. The distinction between the two types of properties is, according to the present authors, more due to historical reasons than of a fundamental character.

An understanding of the thermodynamic properties of a system and the reactions involved in a materials process is essential during modelling. Heat, mass and momentum transfer computations need access to accurate thermophysical data such as viscosities and thermal conductivities. If there are relationships existing between the two types of properties, it is essential that there are mutual compatibilities between the data used for the description of the same process. In other words, in order to have reliable simulation models for materials processes, reliability and compatibility between data used in databases need to be established which, in turn, require a deeper understanding of the relationships between the different properties.

In a survey carried out by the European Space Agency[1], in connection with a project on measurements of thermophysical properties, the European industries expressed a strong need for accurate and reliable thermophysical data for characterizing materials with reference to silicate melts. Among the specific properties identified as highly important are viscosities and thermal diffusivities.

The present paper focuses on the understanding of the thermophysical properties of silicate melts. An attempt is made to present an elucidation of the inter-property correlations by linking up viscosities and thermodynamic properties. A possible coupling between thermal diffusivities and thermodynamic properties, as well as densities and thermodynamic properties, are also examined.

Relationship between viscosity and thermodynamics

Born and Green[2] suggested that the viscosities of liquids may be considered to consist of two parts, i.e. interatomic forces as well as thermal motion. It is a well-known fact that the interatomic/interionic forces leading to viscous flow depends upon the bond strengths between the species

in the system. In the case of silicate melts, the highly polymerized silicate melts have high viscosities. The silicate network breaks down as the basic oxides are added, and the viscosity decreases rapidly.

When studying the mechanism for viscous flow, it can be expected that the viscosity is dependent upon the nearest-neighbour interactions, as well as, the coordination numbers. In fact, the interionic forces in slags are characterized by the thermodynamic state of the system. The enthalpy term is a measure of the interatomic bonding, while the entropy term represents the disorder. In other words, when considering the relationship between the enthalpy and entropy terms, i.e.:

$$\Delta G = \Delta H - T \cdot \Delta S \qquad [1]$$

The Gibbs energy of the system is likely to have a strong influence on the viscosities at a given temperature.

It should be pointed out that viscosity is also a dynamic property, dependent on the motion of the species under shear stress, which, in turn, is influenced by the thermal motion in the liquid in accordance with the suggestion of Born and Green[2]. The thermal motion of a system can be related to the entropy at a given temperature and, thus, indirectly related to the thermodynamic state of the liquid. In other words, the thermodynamics of the liquid silicate may have a strong impact on the viscous flow of these melts.

In the case of silicate melts, even the next-nearest-neighbour interactions, as for example interactions between two cations, may have an influence on the thermodynamic properties as well as, the viscous flow. Richardson[3] has suggested that liquid silicates, with identical MO/SiO_2 ratios, will mix ideally. This would mean that the O^{2-} ions in the silicates are strongly bonded to Si^{4+} cations and that the metal cations are randomly oriented in the oxygen matrix. On the other hand, the sizes and charges of the metal cations would have a polarizing influence on the oxygen matrix, resulting in deviations from ideality. A corresponding effect may be envisaged in the case of viscous flow of silicate melts. Considering the complexity of the interionic interactions in the silicate melt, a simple relationship between the thermodynamics and viscous flow may not be expected.

In the case of metallic melts, Seetharaman and Du Sichen[4] suggested that the second derivative of ΔG^*_{Mix} (the non-linear part of the activation energy for viscous flow in a binary system) with respect to composition is related to the second derivative of the integral molar Gibbs energy for mixing, ΔG^M, with respect to composition according to the following equation:

$$\left[d^2\Delta G^*_{mix} / dX^2\right]_{P,T} = \left[d^2\Delta G^M / dX^2\right]_{P,T} - 6 \cdot R \cdot T \qquad [2]$$

where R is the gas constant in $J \cdot K^{-1} \cdot mol^{-1}$ and T the temperature of the melt. Equation [2] yields, upon integration, the following relationship:

$$\Delta G^*_{mix} - \Delta G^M = 3 \cdot R \cdot T \cdot X_1 \cdot X_2 \qquad [3]$$

Since it has earlier been established that viscous flow is related to the thermodynamic state of the system, the degrees of freedom that affect the integral molar Gibbs energy of a system should even have an impact on the viscous flow of the liquid, which can also be considered as an integral molar property. The classic Maxwell's equation describing the change in the Gibbs energy is expressed as follows:

$$dG = V\,dp - SdT + \sum \mu_i\,dn_i \qquad [4]$$

At constant pressure, the temperature and composition are the two variables that could account for the variation of the Gibbs energy of a system. Since the activation energy for viscous flow is related to the thermodynamic state of the system, it should be possible to analyse viscosity in terms of the same variables.

In other words, if the energetics of viscous flow are analogous to the thermodynamic properties, the changes in Gibbs energies due to strong interactions between various species in the system should be reflected in viscosity as well. Darken[5] has shown that the second derivative of the excess Gibbs energy of mixing with respect to composition in the case of a binary metallic system, termed 'excess stability', should reflect the tendencies for compound formation. The validity of this theory was illustrated in the case of a number of binary metallic systems. Darken[5] applied the excess stability concept to even silicate systems like $CaO\text{-}SiO_2$ and $FeO\text{-}SiO_2$, and thereby showed that the excess stability diagram for these systems revelled peaks corresponding to the formation of stoichiometric compounds. In other words, the second derivative of the logarithm of the viscosity, with respect to composition, has proven to be a sensitive function that would reflect the associations in the liquid silicate melts.

In order to see if the above reasoning, with respect to the second derivative of the viscosities, is valid for other binary silicate melts, attempts were made in the present study to carry out similar calculations. The calculations of the second derivatives of ln η as a function of composition were calculated based on the results obtained for the viscosities of several silicate systems, i.e. $CaO\text{-}SiO_2$, MgO-

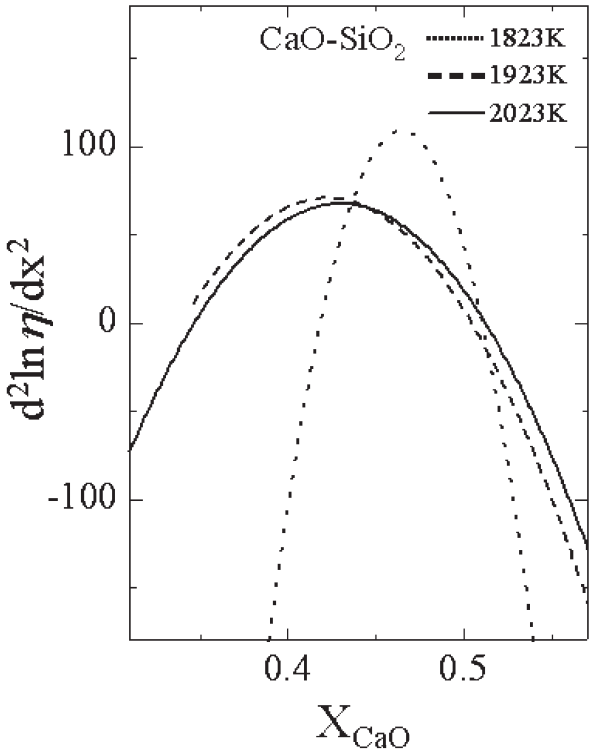

Figure 1. System $CaO\text{-}SiO_2$; the second derivative of ln η with respect to the composition of CaO has been plotted for the following temperatures: 1823 K, 1923 K and 2023 K

SiO_2, MnO-SiO_2, FeO-SiO_2 and Al_2O_3-SiO_2, using the THERMOSLAG® software program. The viscosity data calculated in the present study were in good agreements with the measured viscosities reported in literature[6-20].

The second derivative of ln η as a function of composition of CaO for the system CaO-SiO_2 is presented in Figure 1. In the composition region where the measurements of viscosities have been carried out, it is seen in Figure 1 that the second derivative shows a distinct peak at approximately the equimolar composition, indicating the ionic associations between Ca^{2+} and SiO_3^{2-}, corresponding to the metasilicate. It is also seen that the height of this peak decreases somewhat with the increase in temperature, indicating the effect of entropy on the ionic associations. The slight shift in the peak position could be accounted for by experimental scatter as measurement compositions have to be closer to get a better resolution. The peak corresponding to the $CaSiO_3$ composition is not as pronounced as in the case of the viscosities.

The second derivative of ln η as a function of composition of MgO for the system MgO-SiO_2 is presented in Figure 3. The viscosity measurements have in this case been carried out in a limited range. It is seen from this figure, however, that the plot exhibits a peak corresponding to the composition $MgSiO_3$, which is the metasilicate.

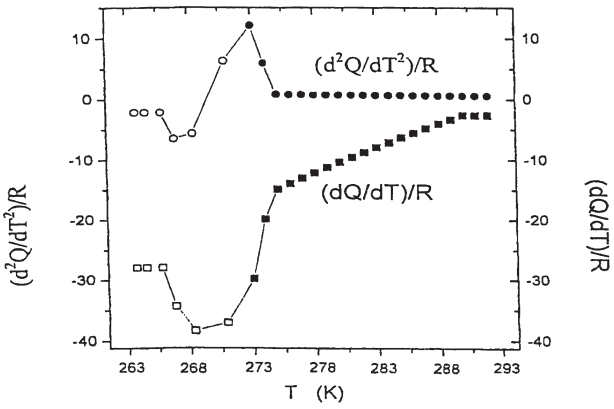

Figure 2. The first and second derivatives of the activation energies for viscous flow for pure water[21]

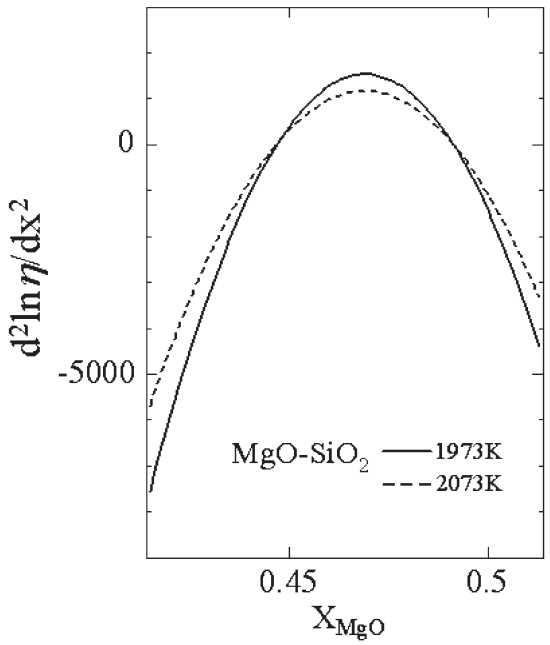

Figure 3. System MgO-SiO_2; the second derivative of ln η with respect to the composition of MgO has been plotted for the following temperatures: 1973 K and 2073 K

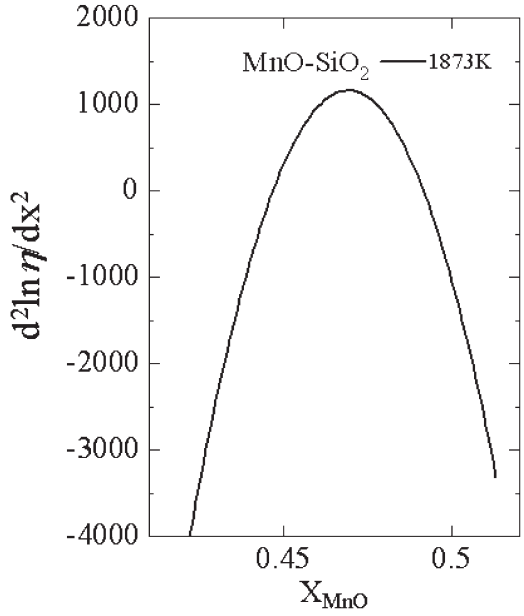

Figure 4. System MnO-SiO_2; the second derivative of ln η with respect to the composition of MnO has been plotted for the following temperature: 1873 K

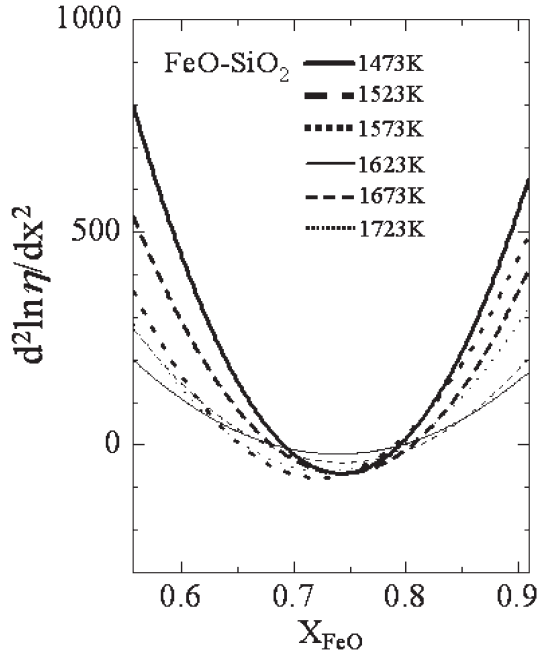

Figure 5. System FeO-SiO_2; the second derivative of ln η with respect to the composition of FeO has been plotted for the following temperatures: 1473 K, 1523 K, 1573 K, 1623K, 1673 K and 1723 K

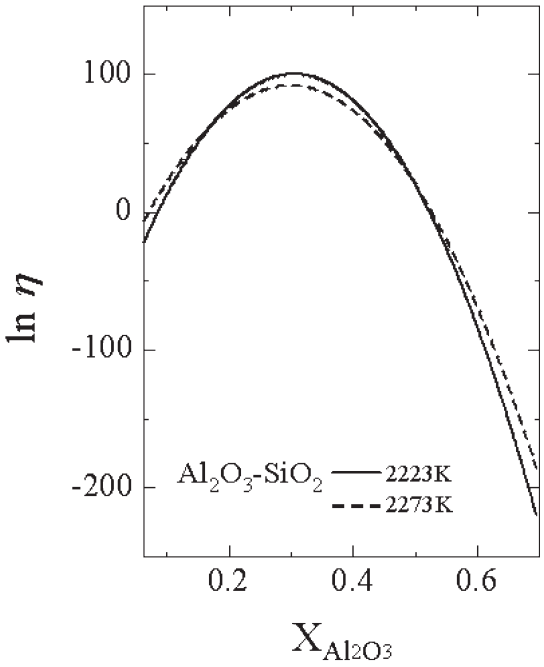

Figure 6. System Al_2O_3-SiO_2; The second derivative of ln η with respect to the composition of Al_2O_3 has been plotted for the following temperatures: 2223 K and 2273 K

The viscosities of the systems MnO-SiO_2, FeO-SiO_2 and Al_2O_3-SiO_2 were also subjected to similar analysis as above. The corresponding curves are shown in Figures 4–6. In all the cases, the second derivative analyses exhibit extrema when plotted as a function of composition, indicating strong ionic associations corresponding to the compound formation in the solid state. In the case of FeO-SiO_2, it can be seen from Figure 4 that the second derivative is, unlike the other systems, a minima. An explanation for the discrepancy between FeO-SiO_2 and the other systems is not clear at this point. It is noteworthy, however, that the temperature regime where viscosity data were available was relatively low for this system, i.e. 1423 K–1723 K and the minima appears to get less pronounced with increasing temperature. It is possible that the minima is connected to the lowered stability of FeO-SiO_2 metasilicate at low temperatures.

Relationships between thermal diffusity and thermodynamics

The structure dependency of the thermal conductivities of silicates has been demonstrated in literature. According to Mills[22] the NBO/T ratio, i.e. the number of non-bridging oxygen atoms per tetrahedrally coordinated atom, for the system CaO-Al_2O_3-SiO_2 is a linear function of the thermal diffusivities. In order to see if this reasoning is valid, attempts were made in the present study to measure thermal diffusivity, by a three-layered laser flash method[23-24], for five compositions in the CaO-Al_2O_3-SiO_2 system. In Table I the chemical compositions of the samples investigated are presented.

The temperature dependencies of the effective thermal diffusivity for two different slag samples with constant $CaO/AlO_{1.5}$ ratio of 1.3 and 2.2 respectively, is presented in Figures 7 and 8. The error bars seen in the figures represent the standard deviation of the experimental values. It is important to point out that the effective thermal diffusivity obtained by the laser-flash method contains the contribution of the radiative heat transfer mechanism. It has been reported, however, that the CaO-Al_2O_3-SiO_2 liquid slags can be successfully regarded as a transparent body irrespective of composition[25]. Due to this, and the fact that all measurements were carried out for the same sample thickness, it can be assumed that the radiation effects on the effective thermal diffusivity are the same for all the CaO-Al_2O_3-SiO_2 slag samples at the same measurement temperature. It can also be assumed that the difference in

Table I
Chemical compositions of the CaO-Al_2O_3-SiO_2 slag samples

Slag	$AlO_{1.5}$	SiO_2	CaO	$X_{CaO}/X_{AlO_{1.5}}$
1	0.15	0.52	0.33	2.2
2	0.23	0.47	0.30	1.3
3	0.18	0.42	0.40	2.2
4	0.27	0.38	0.35	1.3
5	0.33	0.35	0.32	1.0

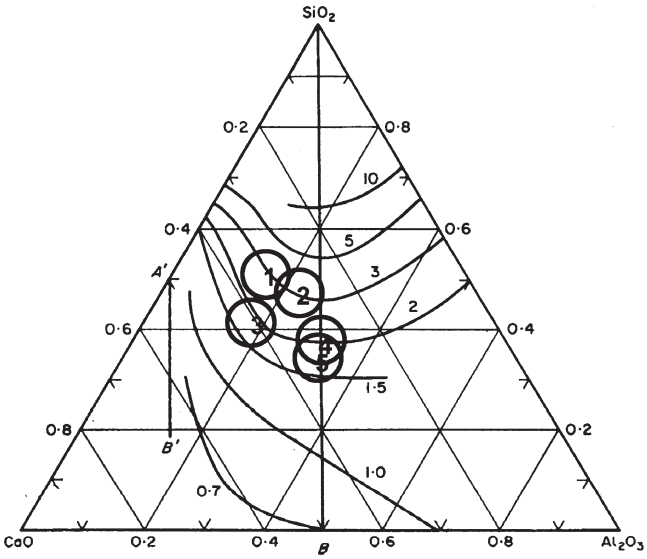

Figure 7. Viscosities in the CaO-A1$_2$-SiO_2 system/25. The numbers within the open circles denote the slag compositions in Table I

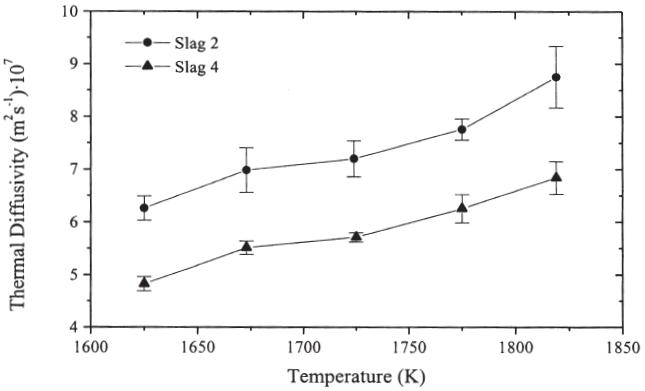

Figure 8. Temperature dependences of the effective thermal diffusivity for slags 2 and 4

the effective thermal diffusivity corresponds to the difference in the phonon thermal diffusivity reflecting the structure.

As can be seen from Figure 7, the effective thermal diffusivity, of slag 2 and 4, increases with an increase in the content of SiO_2. This result is in agreement with the empirical relationship proposed by Mills[22] for the CaO-Al_2O_3-SiO_2 system, i.e. that the thermal conductivity of silicates increases with a decrease in the NBO/T ratio. On the other hand, as shown in Figure 8, slags 1 and 3 exhibits somewhat of the same effective thermal diffusivities in spite of their different SiO_2 content, i.e. different NBO/T ratio. Due to this, it is considered in the present study that for the slag samples having a $CaO/AlO_{1.5}$ ratio of 2.2 or higher, the phonon mean free path is not affected by the structure as the silicate network is dominantly broken down. As a result of this, it can be concluded that the thermal diffusivity is not significantly dependent on the content of SiO_2 , i.e. the NBO/T ratio.

In Figure 9 the temperature dependence of the effective thermal diffusivities of slags 1 and 5 is presented. From Table I it can be seen that slags 1 and 5 have similar contents of CaO, but different ratios of $AlO_{1.5}/SiO_2$. As can be seen from Figure 9, it is found that slag 5, having the higher ratio of $AlO_{1.5}/SiO_2$, exhibits higher thermal diffusivity values than slag 1. For the slag compositions investigated in the present study, it can be assumed that there are enough numbers of non-bridging oxygen ions so that $AlO_{1.5}$ are allowed to behave as a network-forming oxide. However, when $AlO_{1.5}$ behaves as a network-forming oxide, the Ca^{2+} ions are consumed to compensate the charge of Al^{3+} ions, which results in polymerisation. Due to this, it can also be assumed that the polymerization of the silicate network caused by the substitution of $AlO_{1.5}$ for SiO_2 yields an increase of the thermal diffusivity.

The comprehensive analyses of the empirical relationship proposed by Mills[22] has been supported by the effective thermal diffusivity data obtained in the present study for CaO-Al_2O_3-SiO_2 liquid slags. On the other hand, it has also been shown that for slags having higher $CaO/AlO_{1.5}$ ratios, the effective thermal diffusivity is somewhat constant, irrespective of the different ratios of NBO/T. This result implies that when the silicate network is dominantly broken down, the phonon mean free path is not affected by the structure, and the thermal diffusivity is not significantly dependent on the ratio of NBO/T. However, since the thermal diffusivity is relevant to the structure, a relationship should exist, at least for acidic slags, between the thermodynamic properties and thermal diffusivity. Attempts to find such a relationship is currently in progress at the Division of Metallurgy, Royal Institute of Technology (KTH), Stockholm, Sweden.

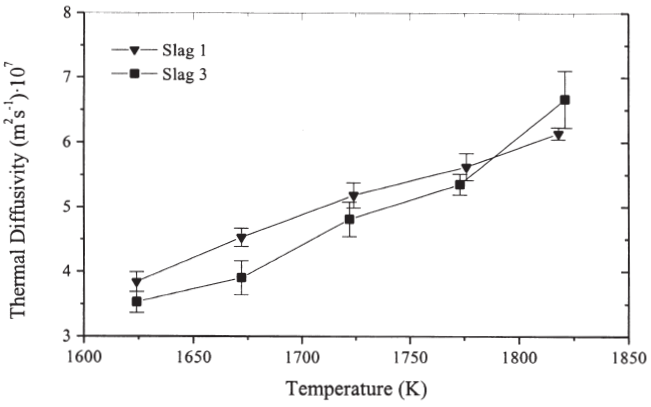

Figure 9. Temperature dependences of the effective thermal diffusivity for slags 1 and 3

Relationship between densities and thermodynamics

As mentioned earlier in the present paper, the thermodynamics of silicate melts not only depend upon the nearest-neighbour interactions, but also the next-nearest neighbour interactions. The integral molar enthalpies of mixing of silicates, as well as the densities (molar volumes) should, in view of this, also be dependent on the interactions. Exothermic enthalpies are indicative of attractive forces, which even may result in volume shrinkage. Based on this reasoning, an attempt was made in the present study to develop a relationship between the enthalpies of mixing and the integral molar volume.

By using the following equation:

$$\frac{V^M}{\sum_i x_i V_i} = \lambda \frac{H^M}{RT} \qquad [5]$$

The integral molar volumes of different silicate melts can be calculated from the enthalpies of mixing and compared with the data for molar volumes obtained from literature. In Equation [5], V^M represents the integral molar volume of the silicate, H^M is the integral molar enthalpies of mixing, $\Sigma x_i V_i$ the average molar volume, R the gas constant, T the temperature and λ is a constant.

From the Gibbs-Helmholtz equation:

$$H^M = \frac{\partial\left(G^M / T\right)}{\partial(1/T)} \qquad [6]$$

where G^M is the integral molar Gibbs energy of mixing, the enthalpies of mixing can be derived. According to Björkvall *et al.*[26], G^M can be expressed as follows:

$$G^M = RTp\sum\left(y_{Ci}\ln y_{Ci}\right) + f\left(T, y_{Si^{4+}}\right) + \sum_{i=1,m-1}\left(\sum_{j=i+1,m} y_{Ci}y_{CJ}\Omega^{Ci,Cj(O)}\right) \qquad [7]$$

where y_{Ci} is the ionic fraction of cation i within the cation grouping defined as:

$$y_{Ci} = \frac{N_{Ci}}{\sum_{j=1}^{m} N_{Cj}} \qquad [8]$$

and the interaction variables as:

$$\Omega^{Ci,Cj(O)} = \Omega_1{}^{Ci,Cj(O)} + \Omega_2{}^{Ci,Cj(O)}T + \left(\Omega_3{}^{Ci,Cj(O)} + \Omega_4{}^{Ci,Cj(O)}T\right)\left(y_{Ci} - y_{Cj}\right) + \left(\Omega_5{}^{Ci,Cj(O)} + \Omega_6{}^{Ci,Cj(O)}T\right)\left(y_{Ci} - y_{Cj}\right)^2 + \cdots \qquad [9]$$

It should be pointed out that when $y_{Si}{}^{4+} \le \frac{1}{3}$ the following is valid for f(T,$y_{Si}{}^{4+}$) in Equation [7]:

$$f\left(T, y_{Si^{4+}}\right) = 0 \qquad [10]$$

However, when $y_{Si}{}^{4+} \ge \frac{1}{3}$ the following is valid:

$$f\left(T, y_{Si^{4+}}\right) = A \cdot \left(y^*_{Si} - y_{Si}\right)^3 \qquad [11]$$

where $y_{Si}^{*}=\frac{1}{3}$, $A=\frac{-\Delta G_L}{\left(y_{Si}^{*}-1\right)^3}$ and $\Delta G_L = 35600 - 7.53T$ (J/mol) (ΔG_L is the change of Gibbs energy for fusion of silica).

When combing Equation [6] with Equation [7] the following relationship is obtained for the enthalpies of mixing:

$$H^M = \frac{\partial\left[f\left(T, y_{Si^{4+}}\right)/T\right]}{\partial(1/T)} + \frac{\partial}{\partial(1/T)} \quad [12]$$

The $\Omega^{Ci,Cj(O)}$ values adopted for the $CaO\text{-}SiO_2$, $FeO\text{-}SiO_2$ and $Al_2O_3\text{-}SiO_2$ systems are summarized in Table II[27].

From Equations [5] and [12] the integral molar volume, V^M, can be calculated. The excess molar volume, V^E, which is equal to V^M, is related to the molar volume of molten slags, V_m, as follows:

$$V^E = V^M = V_m - \sum_i x_i V_{m,i} \quad [13]$$

where $V_{m,i}$ denotes the molar volume of pure i. As a result of this, V_m can be calculated from V^M. On the other hand, V_m can also be obtained from the experimental density through the following relationship:

$$V_m = \frac{\sum_i x_i M_i}{\rho} \quad [14]$$

where ρ is the density, x_i and M_i the mole fraction and the mass per mole for the component *i*, respectively.

In Figures 10 and 11 comparisons between the calculated and experimental values of the integral molar volume of the $CaO\text{-}SiO_2$ system at 1873 K, as well as the $FeO\text{-}SiO_2$ system at 1573 and 1673 K are presented[28-29]. In these cases a value of 0.11 have been adopted for the constant λ in Equation [5] for both systems. It can be seen from the

Table II
Binary interactions variables used in the model calculations[27]

Variable	Expression
$\Omega^{CaSi(O)}$	$-42988.5-113.356T+(-414694+145.133T)(y_{Ca}-y_{Si})-37739(y_{Ca}-y_{Si})^2$
$\Omega^{FeSi(O)}$	$-17609.3-30373.2(y_{Fe}-y_{Si})+36090.7(y_{Fe}-y_{Si})^2$
$\Omega^{AlSi(O)}$	$-10256.9+27248.2(y_{Al}-y_{Si})-10811.9(y_{Al}-y_{Si})^2$

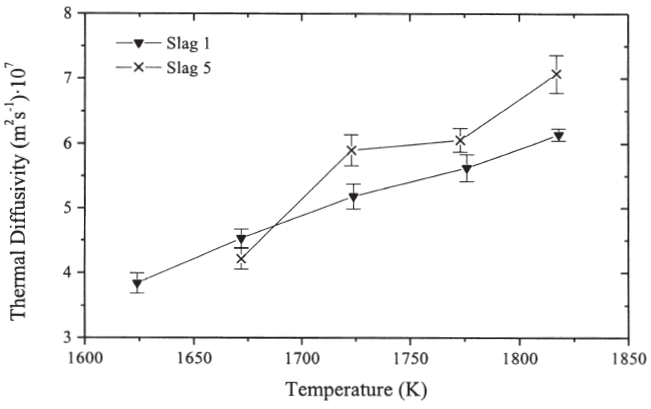

Figure 10. Temperature dependences of the effective thermal diffusivity for slags 1 and 5

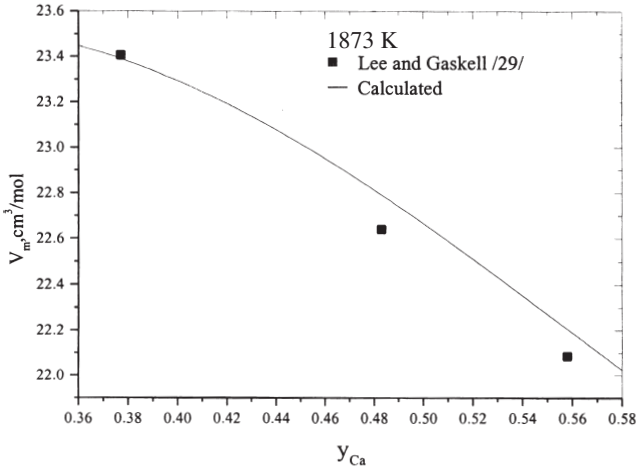

Figure 11. Comparison of calculated and measured molar volume values for the $CaO\text{-}SiO_2$ system at 1873K

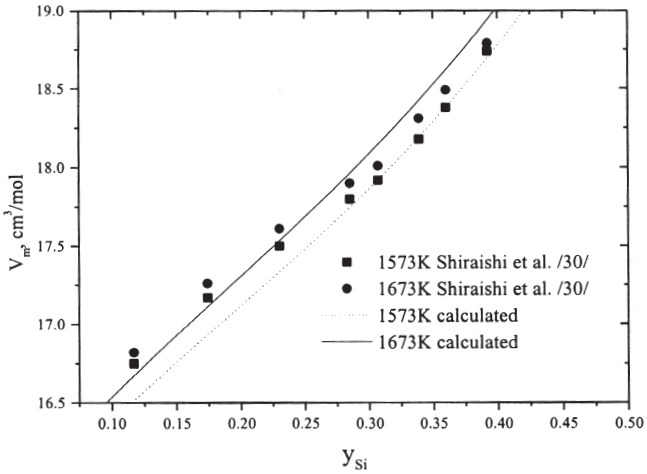

Figure 12. Comparison of calculated and measured molar volume values for the $FeO\text{-}SiO_2$ system at 1573K and 1673K

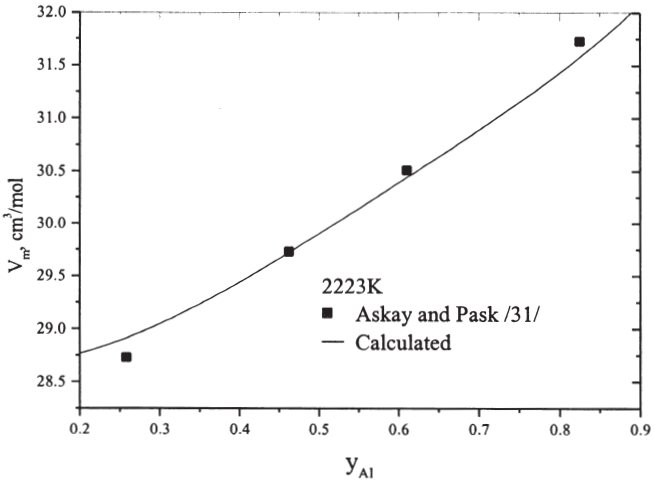

Figure 13. Comparison of calculated and measured molar volume values for the $Al_2O_3\text{-}SiO_2$ system at 2223K

figures that $\lambda = 0.11$ seems to give a good correlation between experimentally obtained V_m and H_M values and those calculated using Equation [12]. For the Al_2O_3-SiO_2 system, however, $\lambda = 0.11$ does not give a good correlation. In this case a value of 0.055 for the constant λ has proven to give a better correlation between the calculated and measured V_m values[30] for the Al_2O_3-SiO_2 system at 2223 K, see Figure 12.

The comparisons between the calculated and experimental values of the integral molar volume, presented in Figures 10–12, do show a slight trend indicating that an intrinsic and quantitative relationship may exist between V_m and H^M in molten oxide systems. As can also be seen from the figures, the scale on the y-axis in the case of the Al_2O_3-SiO_2 system is half of that for the CaO-SiO_2 and FeO-SiO_2 systems. This might be due to structural reasons. However, this viewpoint needs to be further investigated by testing other systems such as Al_2O_3-BO_m or A_2O_m-SiO_2.

Summary

Thermodynamic approaches to the description of viscosities, thermal diffusivities, and densities have been presented in the present study. The results obtained clearly indicate the usefulness of a thermodynamic approach when modelling different physical properties of high temperature silicate melts. Some discrepancies/uncertainties were, however, observed and these are currently being investigated at the Division of Metallurgy, KTH.

References

1. *THERMOLAB Project*, European Space Agency, Noordwijk, Holland, 2001.
2. BORN, M. and GREEN, H. S. *A General Kinetic Theory of Liquid*, Cambridge University Press, London, UK, 1949.
3. RICHARDSON, F. D. *Physical Chemistry of Melts in Metallurgy*, Academic Press, London, UK, vol. 1, 1974. p. 24.
4. SEETHARAMAN, S. and SICHEN, Du. *Metall. Mater. Trans*., vol. 25B, 1994. p. 589.
5. DARKEN, L. S. *TMS-AIME*, vol. 239, 1967. p. 80
6. BOCKRIS, J. O. M. and LOWE, D. C. *Proc. R. Soc*., London, Ser., 1954. p. 423.
7. KOZAKEVITCH, P. P. *Rev. Metaall.*, vol. 57, 1960. p. 149.
8. URBAIN, G. *Rev. Int. Hautes Temp. Refract*., vol. 11, 1974. p. 133.
9. URBAIN, G., BOTTINGA, Y. and RICHET, P. *Geochim. Cosmochim. Acta*, vol. 46, 1982. p. 1061.
10. ENDELL, V. K. and GUNTHER. *Archiv. Eisehuttenw*., vol. 10, 1936. p. 85.
11. JI, F. -Z., SICHEN, DU and SEETHARAMAN, S. *Met. Mat. Trans*. B, vol. 28, 1997. p. 827.
12. BOCKRIS, J. O. M., MACKENZIE, J. D. and KITCHENER, J. A. *Trans Faraday Soc*., vol. 57, 1955. p. 1734.
13. MOFMANN, E. A. *Berg. Huttenmann Monatsh*, vol. 106, 1959. p. 397.
14. RIEBLING, E. F. *Canada J. Chem*., vol. 42, 1964. p. 2811.
15. KAVAI, Y. *Nippon KinzokuGakkai Kaiho*, vol. 18, 1979. p. 224.
16. YAGI, S., MIZOGUCHI, K. and SUGINOHARA, Y. *Kyushu Kogyo Daigaku'*, Hokoku, Kogaku, vol. 40, 1980. p. 33.
17. SOKOLOV, V. I., POPEL, S. I. and ESIN, O. A. *Izv. VUZ Chern. Met*., no. 4, 1970. p. 40.
18. SEGERS, L., FONTANA, A. and WINARD, R. *Electrochim. Acta*, vol. 24, 1979. p. 213.
19. KOZAKEVOTCH, P. P. *Rev. Metallurgie*, vol. XLVI, 1949. p. 505.
20. RÖNTGEN, P., WINTERHAGER, H. and KAMMEL, R. *Erzmetall*, vol. 9, 1956. p. 207.
21. SEETHARAMAN, S., SRIDHAR, S., SICHEN, DU and MILLS, K. C. *Metall. Mater. Trans*., vol. 21B, 2000. p. 111.
22. MILLS, K. C. *ISIJ International*, vol. 33, 1993. p. 148
23. ERIKSSON, R. and SEETHARAMAN, S. *Met. Mat. Trans*. B, In press, 2002.
24. ERIKSSON, R., HAYASHI, M. and SEETHARAMAN, S. *Inter. J. Thermophys*., vol. 24, 2003. p. 785.
25. RICHARDSON, F. D. *Physical Chemistry of Melts in Metallurgy*, Academic Press, London, UK, vol. 1, 1974. p. 107.
26. WASEDA, Y., MASUDA, M., WATANABE, K., SHIBATA, H., OHTA, H. and NAKAJIMA, K. *High temp. Mater. Proc.*, vol. 13, 1994. p. 267.
27. BJÖRKVALL, J., SICHEN, DU and SEETHARAMAN, S. *High Temp. Mater. and Proc.*, vol. 18, 1999. p. 253.
28. BJÖRKVALL, J. *Ph.D. thesis*, Royal Institute of Technology, Stockholm, 2000. p. 56.
29. LEE, Y. E. and GASKELL, D. *R. Metall. Trans*., vol. 5, 1974. p. 853.
30. SHIRAISHI, Y., IKEDA, K., TAMURA, A. and SAITO, T. *Trans. JIM*, vol. 19, 1978. p. 264.
31. ASKAY, I. A. and PASK, J. A. J. *Am. Ceram. Soc*., vol. 62, 1979. p. 332.

Appendix 1: Raw data (viscosity)

The data presented in this appendix have been calculated using the THERMOSLAG® software program developed at the Division of Metallurgy at the Royal Institute of Technology (KTH), Stockholm, Sweden.

Reference

1. SICHEN, D., BYGDEN, J. and SEETHARAMAN, S. *Met. Mat. Trans*. B, vol. 25B, 1994. p. 1.

Table I
Viscosity data for the system $CaO-SiO_2$

Temp (K)	X_{CaO}	Viscosity (Pa.s)
1823	0.1000	5.05E+04
1823	0.2000	3.12E+02
1823	0.3000	8.60E+00
1823	0.4000	8.60E-01
1823	0.5000	2.54E-01
1823	0.6000	1.80E-01
1823	0.7000	2.51E-01
1823	0.8000	5.54E-01
1823	0.9000	1.59E+00

Temp (K)	X_{CaO}	Viscosity (Pa.s)
1923	0.1000	1.28E+04
1923	0.2000	1.12E+02
1923	0.3000	3.96E+00
1923	0.4000	4.71E-01
1923	0.5000	1.54E-01
1923	0.6000	1.15E-01
1923	0.7000	1.59E-01
1923	0.8000	3.39E-01
1923	0.9000	9.10E-01

Temp (K)	X_{CaO}	Viscosity (Pa.s)
2023	0.1000	3.72E+03
2023	0.2000	4.41E+01
2023	0.3000	1.97E+00
2023	0.4000	2.73E-01
2023	0.5000	9.85E-02
2023	0.6000	7.63E-02
2023	0.7000	1.06E-01
2023	0.8000	2.17E-01
2023	0.9000	5.51E-01

Table II
Viscosity data for the system $MgO-SiO_2$

Temp (K)	X_{MgO}	Viscosity (Pa.s)
1973	0.1000	1.34E+04
1973	0.2000	1.84E+02
1973	0.3000	7.28E+00
1973	0.4000	7.60E-01
1973	0.5000	1.90E-01
1973	0.6000	1.03E-01
1973	0.7000	1.11E-01
1973	0.8000	2.13E-01
1973	0.9000	6.65E-01

Temp (K)	X_{MgO}	Viscosity (Pa.s)
2073	0.1000	4.00E+03
2073	0.2000	7.20E+01
2073	0.3000	3.54E+00
2073	0.4000	4.33E-01
2073	0.5000	1.20E-01
2073	0.6000	6.93E-02
2073	0.7000	7.54E-02
2073	0.8000	1.42E-01
2073	0.9000	4.19E-01

Table III
Viscosity data for the system $MnO-SiO_2$

Temp (K)	X_{MnO}	Viscosity (Pa.s)
1873	0.1000	1.50E+05
1873	0.2000	2.09E+03
1873	0.3000	5.03E+01
1873	0.4000	2.23E+00
1873	0.5000	1.93E-01
1873	0.6000	3.45E-02
1873	0.7000	1.35E-02
1873	0.8000	1.21E-02
1873	0.9000	2.68E-02

Table IV
Viscosity data for the system $FeO-SiO_2$

Temp (K)	X_{FeO}	Viscosity (Pa.s)
1473	0.1000	4.93E+07
1473	0.2000	7.06E+04
1473	0.3000	4.45E+02
1473	0.4000	1.04E+01
1473	0.5000	7.76E-01
1473	0.6000	1.54E-01
1473	0.7000	6.97E-02
1473	0.8000	6.04E-02
1473	0.9000	8.52E-02

Temp (K)	X_{FeO}	Viscosity (Pa.s)
1523	0.1000	1.73E+07
1523	0.2000	3.34E+04
1523	0.3000	2.64E+02
1523	0.4000	7.35E+00
1523	0.5000	6.09E-01
1523	0.6000	1.28E-01
1523	0.7000	5.87E-02
1523	0.8000	4.94E-02
1523	0.9000	6.54E-02

Temp (K)	X_{FeO}	Viscosity (Pa.s)
1573	0.1000	6.50E+06
1573	0.2000	1.65E+04
1573	0.3000	1.63E+02
1573	0.4000	5.28E+00
1573	0.5000	4.86E-01
1573	0.6000	1.08E-01
1573	0.7000	4.99E-02
1573	0.8000	4.09E-02
1573	0.9000	5.10E-02

Temp (K)	X_{FeO}	Viscosity (Pa.s)
1623	0.1000	2.59E+06
1623	0.2000	8.57E+03
1623	0.3000	1.03E+02
1623	0.4000	3.88E+00
1623	0.5000	3.92E-01
1623	0.6000	9.20E-02
1623	0.7000	4.29E-02
1623	0.8000	3.43E-02
1623	0.9000	4.04E-02

Temp (K)	X_{FeO}	Viscosity (Pa.s)
1673	0.1000	1.09E+06
1673	0.2000	4.61E+03
1673	0.3000	6.71E+01
1673	0.4000	2.90E+00
1673	0.5000	3.21E-01
1673	0.6000	7.90E-02
1673	0.7000	3.72E-02
1673	0.8000	2.91E-02
1673	0.9000	3.24E-02

Temp (K)	X_{FeO}	Viscosity (Pa.s)
1723	0.1000	4.83E+05
1723	0.2000	2.58E+03
1723	0.3000	4.48E+01
1723	0.4000	2.20E+00
1723	0.5000	2.66E-01
1723	0.6000	6.85E-02
1723	0.7000	3.26E-02
1723	0.8000	2.49E-02
1723	0.9000	2.64E-02

Table V
Viscosity data for the system Al_2O_3-SiO_2

Temp (K)	X_{Al2O3}	Viscosity (Pa.s)
2223	0.1000	3.42E+01
2223	0.2000	3.47E+00
2223	0.3000	9.16E-01
2223	0.4000	3.36E-01
2223	0.5000	1.75E-01
2223	0.6000	1.28E-01
2223	0.7000	1.15E-01
2223	0.8000	1.10E-01
2223	0.9000	9.27E-02

Temp (K)	X_{Al2O3}	Viscosity (Pa.s)
2273	0.1000	2.16E+01
2273	0.2000	2.37E+00
2273	0.3000	6.59E-01
2273	0.4000	2.52E-01
2273	0.5000	1.35E-01
2273	0.6000	1.00E-01
2273	0.7000	9.19E-02
2273	0.8000	8.91E-02
2273	0.9000	7.75E-02

Appendix 2: Raw data (thermal diffusivity)

The data presented in this appendix have been measured at the Royal Institute of Technology (KTH), Stockholm, Sweden, by using a three-layered laser flash method[1–2]. Five compositions in the CaO-Al_2O_3-SiO_2 system have been investigated.

References

1. ERIKSSON, R. and SEETHARAMAN, S. *Met. Mat. Trans*. B, In press, 2002.
2. ERIKSSON, R., HAYASHI, M. and SEETHARAMAN, S. *Inter. J. Thermophys.*, vol. 24, 2003. p. 785.

Table I
Synthetic slag compositions studied in the present investigation

Slag	$X_{Al_2O_3}$	X_{SiO_2}	X_{CaO}	X_{CaO}/X_{SiO_2}	$X_{CaO}/X_{Al_2O_3}$
1	**0.08**	**0.56**	**0.36**	**0.64**	**4.42**
2	**0.13**	**0.53**	**0.34**	**0.64**	**2.59**
3	**0.10**	**0.47**	**0.44**	**0.93**	**4.42**
4	**0.16**	**0.44**	**0.41**	**0.93**	**2.59**
5	**0.20**	**0.42**	**0.39**	**0.93**	**1.98**

Table II
Measured thermal diffusivity values of Slag 1

	Thermal Diffusivity ($m^2.s^{-1}$)×10^7				
Expt. no. / Temp. (K)	**1624**	**1672**	**1724**	**1776**	**1818**
1	4.09	4.81	5.43	5.63	6.07
2	4.05	4.47	5.12	5.63	6.11
3	3.91	4.47	5.44	5.85	6.20
4	3.78	4.62	5.43	5.41	5.92
5	3.94	4.46	5.27	5.58	6.05
6	3.79	4.58	5.10	5.36	6.24
7	3.77	4.47	5.19	5.36	6.17
8	3.65	4.38	5.27	5.92	6.19
9	3.85	4.57	4.94	5.84	6.19
10	3.58	4.72	5.11	5.78	6.16
11	3.85	4.46	4.81	5.78	6.24
12	-	4.31	5.07	5.38	6.15
Average	3.84	4.53	5.18	5.63	6.14
Standard Deviation	0.155	0.141	0.197	0.208	0.919

Table III
Measured thermal diffusivity values of Slag 2

	Thermal Diffusivity ($m^2.s^{-1}$)×10^7				
Expt. no. / Temp. (K)	**1625**	**1673**	**1724**	**1775**	**1819**
1	6.04	7.77	6.39	7.49	8.39
2	6.07	6.50	6.84	7.55	9.62
3	6.47	6.98	7.30	8.01	9.57
4	6.41	6.44	7.06	7.91	9.48
5	6.25	7.41	7.18	7.85	8.47
6	6.17	7.27	7.87	7.57	9.29
7	5.82	6.41	6.95	7.78	9.00
8	6.24	6.81	6.96	7.66	7.57
9	6.26	7.01	8.32	8.12	8.39
10	6.50	7.08	7.71	7.88	8.89
11	6.61	7.10	6.99	7.60	7.89
12	-	-	7.13	7.67	8.11
Average	6.26	6.98	7.22	7.76	8.72
Standard Deviation	0.231	0.423	0.516	0.199	0.688

Table IV
Measured thermal diffusivity values of Slag 3

	Thermal Diffusivity ($m^2.s^{-1}$)×10^7				
Expt. no. / Temp. (K)	**1624**	**1672**	**1722**	**1773**	**1821**
1	3.37	4.54	5.20	5.53	7.53
2	3.24	4.20	4.97	5.59	6.45
3	3.38	4.02	4.92	5.40	7.42
4	3.48	3.77	4.87	5.34	6.34
5	3.76	3.85	4.95	5.27	6.30
6	3.51	3.83	5.19	5.23	6.41
7	3.59	3.78	4.79	5.14	6.65
8	3.50	3.86	4.36	5.07	6.51
9	3.61	3.72	4.88	5.57	6.42
10	3.68	3.62	4.64	5.37	6.62
11	3.79	3.74	4.55	5.39	-
12	3.47	-	4.44	5.32	-
Average	3.53	3.90	4.81	5.35	6.66
Standard Deviation	0.163	0.263	0.270	0.162	0.440

Table V
Measured thermal diffusivity values of Slag 4

	Thermal Diffusivity ($m^2.s^{-1}$)×10^7				
Expt. no. / Temp. (K)	**1625**	**1673**	**1725**	**1775**	**1819**
1	4.86	5.24	5.62	6.35	7.17
2	5.05	5.50	5.67	6.41	6.93
3	4.86	5.54	5.79	6.47	7.11
4	5.00	5.69	5.77	6.48	7.26
5	4.77	5.60	5.66	6.59	6.97
6	4.83	5.57	5.76	6.42	7.11
7	4.86	5.59	5.69	6.32	7.00
8	4.56	5.30	5.53	5.99	6.55
9	4.63	5.48	5.84	6.12	6.55
10	4.86	5.55	5.77	5.86	6.48
11	4.85	5.47	5.78	5.82	6.47
12	4.80	5.60	5.63	-	6.46
Average	4.83	5.51	5.71	6.26	6.84
Standard Deviation	0.136	0.127	0.089	0.267	0.311

Table VI
Measured thermal diffusivity values of Slag 5

	Thermal Diffusivity ($m^2.s^{-1}$)×10^7			
Expt. no. / Temp. (K)	**1672**	**1723**	**1773**	**1817**
1	3.80	5.61	6.37	6.86
2	4.29	5.66	6.25	7.36
3	4.31	5.99	6.11	6.99
4	4.08	6.09	6.15	7.47
5	4.30	6.04	6.18	7.64
6	4.24	5.92	6.11	7.06
7	4.18	6.44	5.90	6.88
8	4.31	5.92	6.00	6.89
9	4.20	5.75	5.90	6.86
10	4.30	5.73	5.91	7.15
11	4.35	5.76	5.75	7.11
12	-	-	-	6.62
Average	4.22	5.90	6.06	7.07
Standard Deviation	0.159	0.239	0.183	0.292

Appendix 3: Raw data (molar volumes)

The data presented in this appendix have been measured by Lee and Gaskell[1] for the system $CaO\text{-}SiO_2$, Shiraishi *et al.*[2] for the system $FeO\text{-}SiO_2$ and Askay and Pask[3] for the system $Al_2O_3\text{-}SiO_2$.

References

1. LEE, Y. E. and GASKELL, D. R. *Metall. Trans.*, vol. 5, 1974. p. 853.
2. SHIRAISHI, Y., IKEDA, K., TAMURA, A. and SAITO, T. *Trans. JIM*, vol. 19, 1978. p. 264.
3. ASKAY, I. A. and PASK, J. *A. J. Am. Ceram. Soc.*, vol. 62, 1979. p. 332.

Table I
The experimental density and molar volume data of the binary system $CaO\text{-}SiO_2$

x_{CaO}=0.4830			x_{CaO} =0.3770			x_{CaO} =0.5580		
T (K)	**ρ (g/cm^3)**	**V_m, (cm^3/mol)**	**T (K)**	**ρ (g/cm^3)**	**V_m, (cm^3/mol)**	**T (K)**	**ρ (g/cm^3)**	**V_m, (cm^3/mol)**
1873	2.570	22.63	**1840**	2.520	23.24	**1850**	2.630	22.00

Table II
The molar volume data of the binary system $FeO\text{-}SiO_2$

x_{SiO2}	1673 K	1573 K
	V_m (cm^3/mol)	**V_m (cm^3/mol)**
0.1170	16.82	16.75
0.1740	17.26	17.17
0.2300	17.61	17.50
0.2850	17.90	17.80
0.3070	18.01	17.92
0.3390	18.31	18.18
0.3600	18.49	18.38
0.3920	18.79	18.74

Table III
The experimental density and molar volume data of the binary system Al_2O_3 -SiO_2

x_{Al2O3}=0.1482			x_{Al2O3}=0.3008		
T (K)	**ρ (g/cm^3)**	**V_m, (cm^3/mol)**	**T (K)**	**ρ (g/cm^3)**	**V_m, (cm^3/mol)**
2182	2.313	28.66	**2182**	2.448	29.69
2236	2.305	28.76	**2186**	2.449	29.68
2261	2.302	28.80	**2214**	2.445	29.73
2281	2.302	28.80	**2248**	2.446	29.72

x_{Al2O3}=0.4692			x_{Al2O3}=0.7021		
T (K)	**ρ (g/cm^3)**	**V_m, (cm^3/mol)**	**T (K)**	**ρ (g/cm^3)**	**V_m, (cm^3/mol)**
2183	2.625	30.38	**2239**	2.811	31.84
2211	2.615	30.50	**2266**	2.799	31.98
2232	2.612	30.53	**2268**	2.791	32.07
2258	2.608	30.58			